ELSEVIER

Coastal Engineering 47 (2003) 367–379

Coastal Engineering
An International Journal for Coastal, Harbour and Offshore Engineers

www.elsevier.com/locate/coastaleng

Experiments on the reflection coefficients of a detached breakwater in a directional wave field

Wei-Po Huang*, Chun-Ren Chou, John Z. Yim

The Ocean Engineering Laboratory, Department of Harbour and River Engineering, National Taiwan Ocean University, 2, Pei-Ning Road, 20224 Chilung, Taiwan, ROC

Received 20 November 2001; received in revised form 3 September 2002; accepted 20 September 2002

Abstract

Results of estimating the directional wave fields in front of a detached breakwater are presented here in this paper. Two of non-phase-locked methods, i.e., the Maximum Likelihood Method (MLM) and the Extended Maximum Entropy Principle Method (EMEP), were adopted for the purpose. In general, the latter outperforms the former. It is shown that the reflection coefficients decrease with increasing distances away from the detached breakwater, and within four wavelengths from the detached breakwater, the rate of the decrease is faster for wave fields having larger directional spreads. When the measuring distance is more than four wavelengths away from the detached breakwaters, the reflection coefficients tend to reach to a constant value. It is shown that, with the use of the non-phase-locked EMEP method, the effective region can be extended, as compared with the results of Huntley and Davidson [J. Waterw. Port Coast. Ocean Eng. 124 (1998) 312].

Keywords: Reflection coefficient; Directional spectrum; Non-phase-locked

1. Introduction

Due to its importance in the designing and constructing of coastal structures, coastal engineers have been long interested in the determination of the reflection coefficients associated with these structures. In dealing with these problems, the influence of wave directionality has often been neglected in the past.

Basically, most of these methods (Goda and Suzuki, 1976; Gaillard et al., 1980) were simplified by assuming that waves are unidirectional, incident normally to the marine structures, and the reflected waves travel in a direction, which is exactly 180° out of phase with that of the incident waves. Owing to these assumptions, the complexity of the physical process of the reflection in front of a marine structure is largely reduced, and these methods can be implemented with relative ease. However, actual wave fields are directional. The principal wave direction may be dependent on, among others, the prevailing wind direction and the underlying topography. Large oblique angles of the incident waves in front of breakwaters can occur all the time. Under these circumstances, imprecise results can result when the above-mentioned methods are used for the estimation of reflection coefficients.

* Corresponding author. Tel.: +886-2-2463-3684; fax: +886-2-2463-3684.

E-mail address: d87520057@mail.ntou.edu.tw (W.-P. Huang).

0378-3839/02/$ - see front matter
PII: S0378-3839(02)00129-1

In a wave field, where each wave can travel with its own direction, the distribution of wave energy should be estimated using methods suitable for directional seas. Nwogu (1989) has reviewed several methods for estimating the directional wave spectrum, including the Direct Fourier Transform method, the MLM, and the Maximum entropy method (MEM). Basically, all these methods are based on the assumption that the sea state is homogeneous. Furthermore, no components of any two waves are correlated and their phase relationships are not dependent.

However, these assumptions break down near a reflector. There, reflected component waves with the same frequency will be phase-locked to their incident counterparts. At locations in front of a reflector, when the total time needed for a certain component wave to travel to the reflector and back again is a multiple of half the wave period, nodes and antinodes in the form of standing waves will occur. As pointed out by Davidson et al. (2000), if sensors were located at these points, any uncorrelated noise will be interpreted as very large amplitude waves. This will then lead to erroneous estimates of the reflection coefficients. Isobe and Kondo (1984) (see also Kondo et al., 1986; Yokoki and Isobe, 1996) overcame the problem of phase-locking by adding terms to consider the phase interaction between incident and the reflected waves. The method was called the Modified Maximum Likelihood Method (MMLM). It should be noted that, in applying this method, the location of an effective reflection line is needed as prerequisite. However, due to the variability of the wave conditions and the characteristics of coastal structures, the location of the reflection line may become ambiguous in practical conditions.

When wave gauge array is moved away from a reflector toward the sea, the effect of the phase locking is then reduced. However, Davidson et al. (1998) and Huntley and Davidson (1998) have shown that the use of MMLM in these regions will results in spurious peaks in the estimated directional spectra. As pointed out by these authors, this is because that this method gives rise to predicted nodes at sensor locations that are correlated with frequency-direction combinations. As the information of phase locking becomes obscured in these regions, enormous errors in the estimation will occur. These studies have led these authors to propose to divide the wave field in front of a reflector into two regions. Quite near the reflector, a phase-locked estimation method should be used, whereas a non-phase-locked method should be used for regions away it. As a rough estimate, they proposed to the time ratio of L/S, where L is the total time needed for an incident component wave to travel to the reflector and back to the sensor, and S is length of each time segment used in spectral analysis. According to them, non-phase-locked methods, such as MLM, should be used for L/S larger than 0.5.

On the other hand, for the usual methods that do not consider the effect of phase-locking, the presumption of an effective reflection line is not needed (Elgar et al., 1994; Ilic et al., 2000). In these methods, the effect of phase-locking is neglected and incident and reflected waves are treated as independent free waves. It is worth mentioning that the effect of phase-locking can be minimized by increasing the bandwidth in the frequency domain, or through data windowing (Chadwick et al., 1995).

In this paper, measurements have been made in front of a detached breakwater in a laboratory basin. The non-phase-locked methods, the EMEP (Hashimoto et al., 1993) and the MLM were both conducted in estimating the directional spectrum for evaluating the appropriate regions. In the following, the rest of this article is further divided into four parts. In Section 2, a brief description of the adopted mathematical background will be given. Experimental setups are described in Section 3. In Section 4, we demonstrate the superiority of the EMEP in estimating wave fields with reflection when the effects of phase locking are present. With a short summary in Section 5, we then close this paper.

2. Mathematical background

2.1. Definition of the incident and reflected energy

The directional spectrum $S(f,\theta)$ describes the distribution of wave energy in both the spatial and frequency domains. It can be expressed as:

$$S(f,\theta) = S(f) \cdot G(f,\theta) \tag{1}$$

$S(f)$ is the one-sided frequency spectrum which is determined from the record of free-surface elevation.

It does not take the wave directionality into consideration. $G(f,\theta)$ is the spreading function that describes the distribution of the wave energy on their propagation directions from 0 to 2π. Even though the wave energy can be distributed in different directions, the total energy of the wave field should remain unchanged. Therefore, $G(f,\theta)$ should have the following property.

$$\int_0^{2\pi} G(f,\theta)\mathrm{d}\theta = 1 \tag{2}$$

When incident and reflected waves coexist in a wave field, the estimated directional spectrum will be bimodal. Elgar et al. (1994) and Ilic et al. (1997) have shown that the reflection coefficients will vary with frequency and direction bands. Separating the wave field in front of a breakwater into the incident and reflected parts, hereafter denoted as respectively $S_\mathrm{I}(f,\theta_\mathrm{I})$ and $S_\mathrm{R}(f,\theta_\mathrm{R})$, the reflection coefficient K_R can be defined as (Frigaard et al., 1997):

$$K_\mathrm{R}(f,\theta) = \sqrt{\frac{S_\mathrm{R}(f,\theta_\mathrm{R})}{S_\mathrm{I}(f,\theta_\mathrm{I})}} \tag{3}$$

In a laboratory wave basin, waves that are generated by the wave generator, and propagate toward the test model can be considered as incident waves. On the other hand, waves that travel in directions toward the wave generator are considered as reflected waves. These waves are reflected by the test model or from the dissipating beach on the other end of the basin. A definition sketch is shown in Fig. 1, where the experimental setups are also shown. Integrating the directional spectrum in the separated directional bands, i.e., the direction of incident and reflected domain, the reflection coefficient as a function of frequency can be summarized as:

$$K_\mathrm{R}(f) = \sqrt{E_\mathrm{R}(f)/E_\mathrm{I}(f)} \tag{4}$$

where

$$E_\mathrm{I}(f) = \int_{180^\circ}^{360^\circ} S(f,\theta)\mathrm{d}\theta \tag{5}$$

$$E_\mathrm{R}(f) = \int_{0^\circ}^{180^\circ} S(f,\theta)\mathrm{d}\theta \tag{6}$$

are respectively the incident and the reflected wave energies.

2.2. Maximum likelihood method

All currently available methods used to estimate the directional spectrum are based on cross-spectra. These cross-spectra may be the results of either point measurements of different wave properties, or surface fluctuations measured at different locations. The MLM is popularly used because of its simplicity (Brissette, 1992; Chadwick et al., 1995). However, the estimates may sometimes become erroneous. This is especially true when the calculated cross-spectra are inaccurate, or when the wave gauge array is inappropriately arranged. It was originally used in probability theory to estimate the parameters of a probability distribution that maximized the likelihood of obtaining the observed data (Nwogu, 1989).

2.3. Extended maximum entropy principle method

Generally speaking, the Bayesian Directional Spectrum Estimation Method (BDM, Hashimoto et al., 1987) provides the highest resolution in estimating the directional spectrum. Its drawback lies in that it requires a time-consuming iterative computation. The EMEP, first proposed by Hashimoto et al. (1993) retained the advantage of the BDM and decreased the time of iterative refinements. Possible errors contained in the cross-spectra were taken into account, and a Newton's technique of iteration was applied to minimize them.

The formulation of $G(f,\theta)$ estimated by the EMEP is characterized by an exponential function that can be expressed as:

$$G(f,\theta) = \frac{\exp\left[\sum_{n=1}^{M}\left\{a_n(f)\cos n\theta + b_n(f)\sin n\theta\right\}\right]}{\int_0^{2\pi}\exp\left[\sum_{n=1}^{M}\left\{a_n(f)\cos n\theta + b_n(f)\sin n\theta\right\}\right]\mathrm{d}\theta} \tag{7}$$

where $a_n(f)$ and $b_n(f)$ are the unknown parameters and M is the order of the modal. Hashimoto (1997) gave more detailed expressions and discussions concerning procedures of the iterative computation.

The unknown parameters will be calculated by substituting Eqs. (1) and (7) into Eq. (8). The relation-

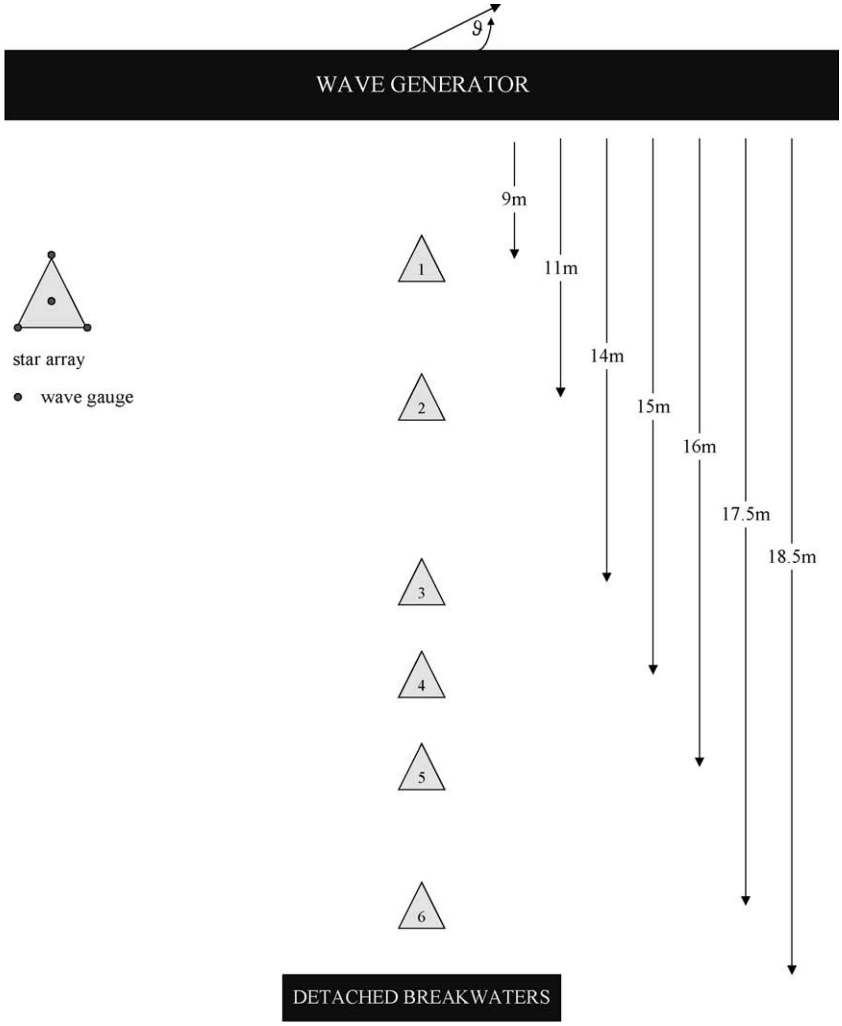

Fig. 1. Set-up of the experiment.

ship between the cross-spectrum and the directional spectrum is expressed as:

$$\phi_{jk} = \int_0^{2\pi} S(f,\theta)\exp\left\{-i\overrightarrow{\mathbf{k}}\cdot\left(\overrightarrow{\mathbf{x}_{jk}}\right)\right\}\mathrm{d}\theta \tag{8}$$

3. Experimental set up

Experiments were carried out in the multi-directional wave basin ($50 \times 50 \times 1$ m) of the Ocean Engineering Laboratory, National Taiwan Ocean University. During the experiments, a water depth of 0.6 m is constantly maintained. A serpentine wave generator of piston type, consisting of 56 paddles is located at one side of the wave basin. A 1:6 gravel beach is paved on the opposite side of the wave generator. Furthermore, mesh sheet wave absorbers are used for the surrounding sidewalls of the basin. Preliminary tests conducted without the detached breakwater have shown that the reflected energies were never more than 5% those of the incident waves. It is believed that experiments with the breakwater were only slightly affected by re-reflection from the sidewalls of the basin.

The detached breakwater was 4 m in length, 0.6 m in width and 0.9 m in height. It was a model of a

Table 1
The experimental condition

Target Spectrum	JONSWAP
Peak frequency	0.6, 0.8, 1.0, 1.2 (Hz)
$H_{1/3}$	5, 8 (cm)
Main wave direction	90°
Spreading index S_{max}	10, 25, 50

standard perpendicular caisson and located at 18.5 m away from the wave generator. To simplify the experiments, none of the wave-dissipating blocks were used in the bottom of the detached breakwaters. The surface of the detached breakwater was smooth and impermeable. The height of the detached breakwater was beyond the general scale to ensure no overtopping. That is to say, there was only slight energy dissipating due to the detached breakwater. To examine the possible effects of the detached breakwaters on the wave field, experiments were conducted for cases both with and without the detached breakwater. Table 1 summarizes the wave conditions used for the experiments.

A sampling rate of 20 Hz was used throughout the experiments. The record length of each experiment was 819.2 s. The data were further divided into 32 segments, each having 512 data points. The calculated auto-, co- and quad-spectra of each segment were then averaged for the directional spectra estimation. The frequency bandwidth was 0.039 Hz. Measurements were conducted using wave gauges in form of the so-called star arrays. The shortest distance between the wave gauges in an array is 30 cm. The shortest wavelength that is detectable by this configuration is therefore 60 cm. A total of six star arrays were used and they were all located in front of the detached breakwater. A definition sketch of the experimental

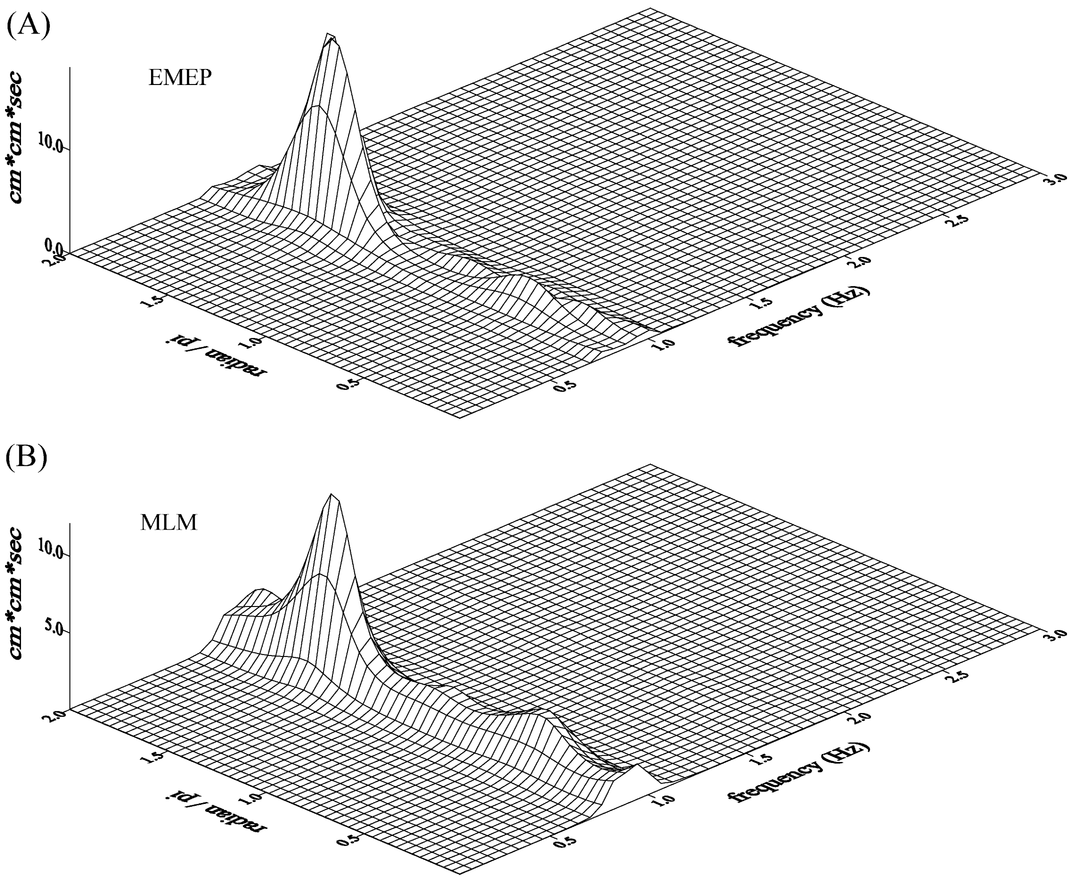

Fig. 2. Directional spectrum estimated by the EMEP and the MLM for the case with $S_{max} = 10$ at the distance of 4.5 m from the breakwater.

setup is shown in Fig. 1. Throughout the experiments, the target spectra are of the JONSWAP type:

$$S(f) = \alpha(2\pi)^{-4} g^2 f^{-5} \exp\left[-\frac{5}{4}\left(\frac{f}{f_p}\right)^{-4}\right] * \gamma^{\exp[-(f/f_p-1)^2/2\sigma^2]} \quad (9)$$

where α is the Phillips constant (≈ 0.081), f_p is the peak frequency, γ is the peak enhancement factor (mean ≈ 3.3).

$$\sigma = 0.07 : f \leq f_p = 0.09 : f > f_p \quad (10)$$

In generating multidirectional waves, a spreading function of the Mitsuyasu type was used (Goda, 2000). To increase degrees of freedom of the spectra estimate as far as possible, the calculated cross and auto spectra were ensemble averaged and Hanning windowed: Eqs. (11)–(13).

$$\phi_i = 0.25\phi_{i-1} + 0.5\phi_i + 0.25\phi_{i+1} \quad (11)$$

where ϕ_i is spectrum density i:2 ~ $n-1$, numbers of the frequency segment and

$$\phi_1 = 0.5\phi_1 + 0.5\phi_2 \quad (12)$$

$$\phi_n = 0.5\phi_{n-1} + 0.5\phi_n \quad (13)$$

4. Results from laboratory experiments

4.1. Effect of spreading parameter

Figs. 2 and 3 show the directional spectra estimated by the EMEP and the MLM for the cases with

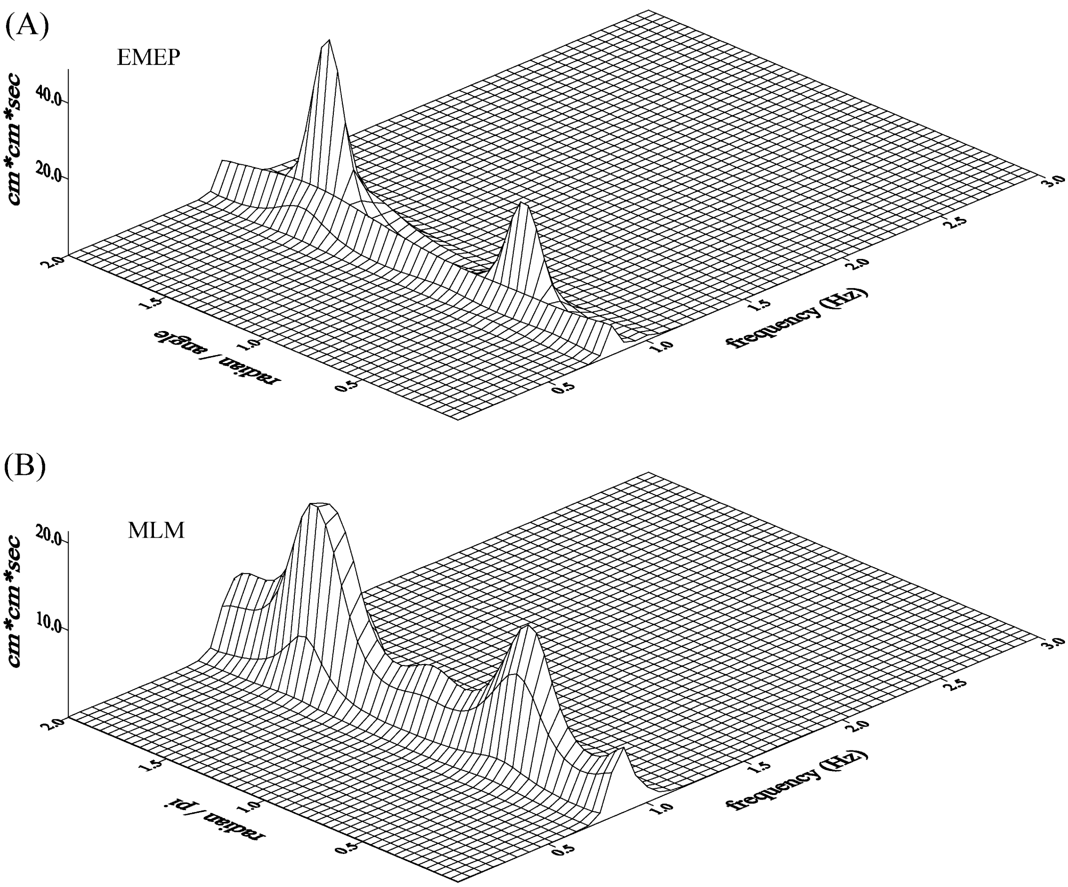

Fig. 3. Directional spectrum estimated by the EMEP and the MLM for the case with $S_{max} = 50$ at the distance of 4.5 m from the breakwater.

spreading parameters S_{max} of the wave field equal to 10 and 50, respectively. The star array is located at 4.5 m in front of the detached breakwater. As pointed out by Goda (2000), with a spreading parameter of $S_{max}=10$, the wave field can be considered as composed mostly of wind waves and the energy of the waves is distributed over all directions. On the other hand, with a spreading parameter of $S_{max}=50$, the wave field is composed mainly of long-crested swell, with highly concentrated energy traveling in a narrow width of azimuth around the principal wave direction. As can be seen from these figures, both methods yield two peaks in the spatial domain. Notice that in these two figures, the abscissas are normalized using ϕ. The reflected waves are located in the region from 0 to 1 of the dimensionless axis, whereas the incident waves are located from 1 to 2.

For the case with $S_{max}=10$ (Fig. 2), the peaks of the reflected waves are small, i.e., only a small portion of the wave energies are reflected. Comparing Fig. 2A and B, it can be seen that the peak value of the reflected spectral energy estimated by the EMEP (Fig. 2A) is larger than that estimated by the MLM (Fig. 2B). Being, respectively, 12.45 $cm^2 \cdot s$ for the former, and 11.12 $cm^2 \cdot s$ for the latter. The directional spectrum estimated by the MLM is flatter, and the energy is dispersed over the entire spatial domain than that due to EMEP. The reflection coefficients estimated by the two methods are 0.51 and 0.69, respectively for EMEP and for MLM.

For the case with $S_{max}=50$, the largest value of the spreading parameter in our experiments, it can be seen from Fig. 3 that a substantial amount of wave energies is reflected. The reflection coefficients estimated by

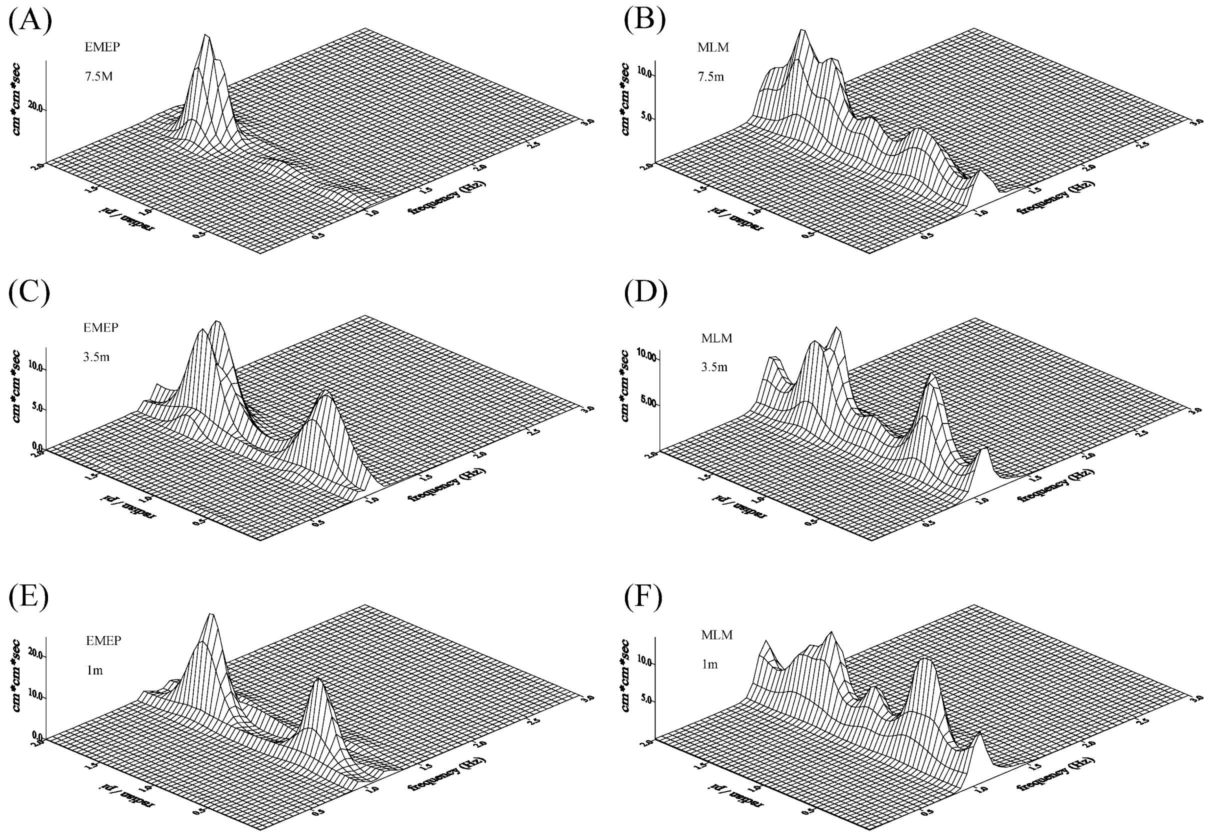

Fig. 4. Directional spectrum estimated by the EMEP and the MLM for the case with $S_{max}=25$, $H_{1/3}=8$ cm, $f_{peak}=1.0$ Hz. (A, C and E) EMEP estimates, (B, D and F) MLM estimates. The distances away from the breakwater are: (A, B) 7.5 m; (C, D) 3.5 m; (E, F) 1 m.

Table 2
The reflection coefficients estimated by the EMEP within the different region of D/WL

D/WL	Numbers of the data sets	S_{max}		
		10	25	50
0–1	36	0.94	0.96	0.99
1–2	27	0.71	0.82	0.87
2–3	27	0.56	0.60	0.65
3–4	27	0.56	0.67	0.52
4–5	9	0.40	0.48	0.41
5–6	9	0.51	0.46	0.46
6–7	9	0.59	0.49	0.40

the EMEP and the MLM are, respectively, 0.74 and 0.83. The distribution of the wave energy estimated by the EMEP is seen to be highly concentrated around the principal direction (Fig. 3A).

It should be mentioned that, except for the values of the spreading parameters, S_{max}, all other experimental conditions are the same for both Figs. 2 and 3. Comparing the results, it can be seen that the reflection coefficients increase with increasing values of the spreading parameter S_{max}. It is well known that with larger values of the spreading index, the waves will be more and more long-crested. This, on the other hand, means that more and more energies are concentrated in the principal direction of wave travel. Briggs et al. (1995) studied the diffraction of a semi-infinite breakwater in a directional wave field. They found that with increasing spreading parameter S_{max}, less and less incident wave energy will be diffracted into the lee of the breakwater. Unfortunately, these authors have not given their estimates of the reflected energies in that paper, so that a direct comparison of our results with those of Briggs et al. (1995) is impossible for the moment. The sum of the reflected, diffracted and dissipated energies should be equal to that of the incident waves. Since the detached breakwater used in the experiments is of vertical type, and has no other

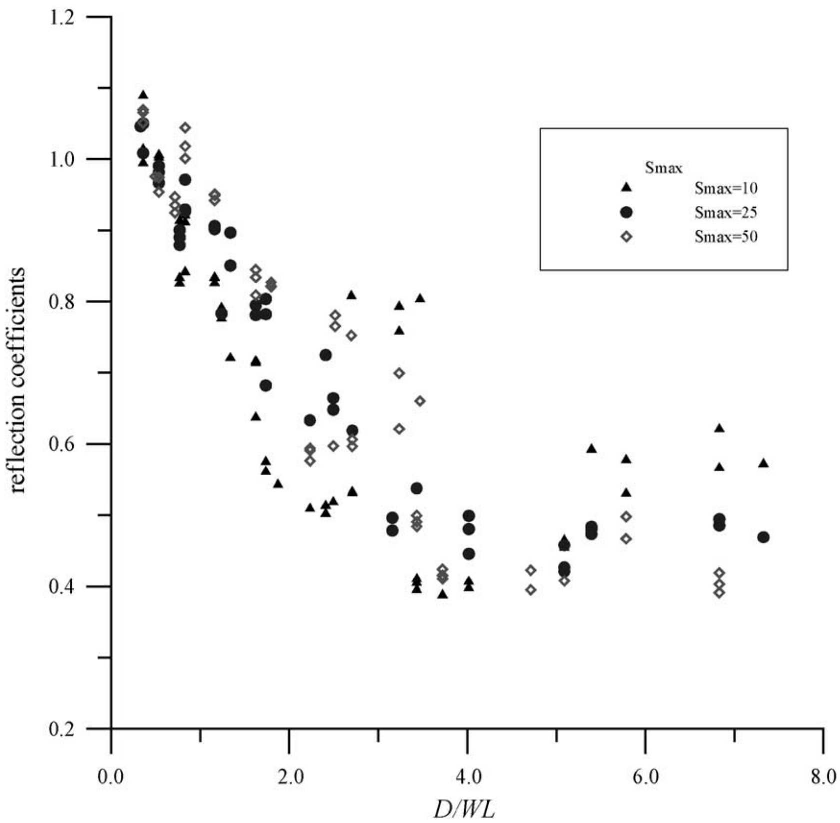

Fig. 5. Reflection coefficients estimated by the EMEP method.

wave dissipation facilities around it, only a small amount of energy can be dissipated through wave breaking. Thus, inferring from the results of Briggs et al. (1995), with a larger spreading parameter, less wave energy will be diffracted, and, as a result, more energies are reflected.

On the other hand, the reflection coefficients estimated by the MLM are larger than those by the EMEP. For the result of MLM, Fig. 3B, there are small humps at the values of 0, 1 and 2 of the dimensionless abscissa that are absent for the result of EMEP (Fig. 3A). This seems to be the inherent drawback of the MLM when used to estimate the spreading function of a bimodal wave field which has a wide spread energy.

4.2. Effect of measuring distance

Fig. 4 shows the directional spectrum estimated by the EMEP and the MLM and the spreading parameter S_{max} of the wave field is 25. The measuring distances (D) between the central wave gauges of each star array to the detached breakwater are, 7.5, 3.5 and 1 m, respectively.

The results of the EMEP, see Fig. 4A, C and E, show that as the distances are decreased, the reflections can be identified more clearly. On the other hand, even though the results of the directional spectral estimates by the MLM can predict the principal direction of the wave propagation correctly, Fig. 4B, D and F, it is also found that wave energies are now distributed irregularly in the spatial domain. It can be seen from Fig. 4B, D and F that, as the measuring stations are located near to the detached breakwater, spurious peaks occurred in the estimated results. The standing waves caused by phase locking are found near the reflector. This has caused the MLM to have difficulties in separating incident and reflected wave energies.

Table 2 summarizes the average reflection coefficients in different regions of D/WL estimated by the EMEP. The ratio of D/WL denotes the measuring

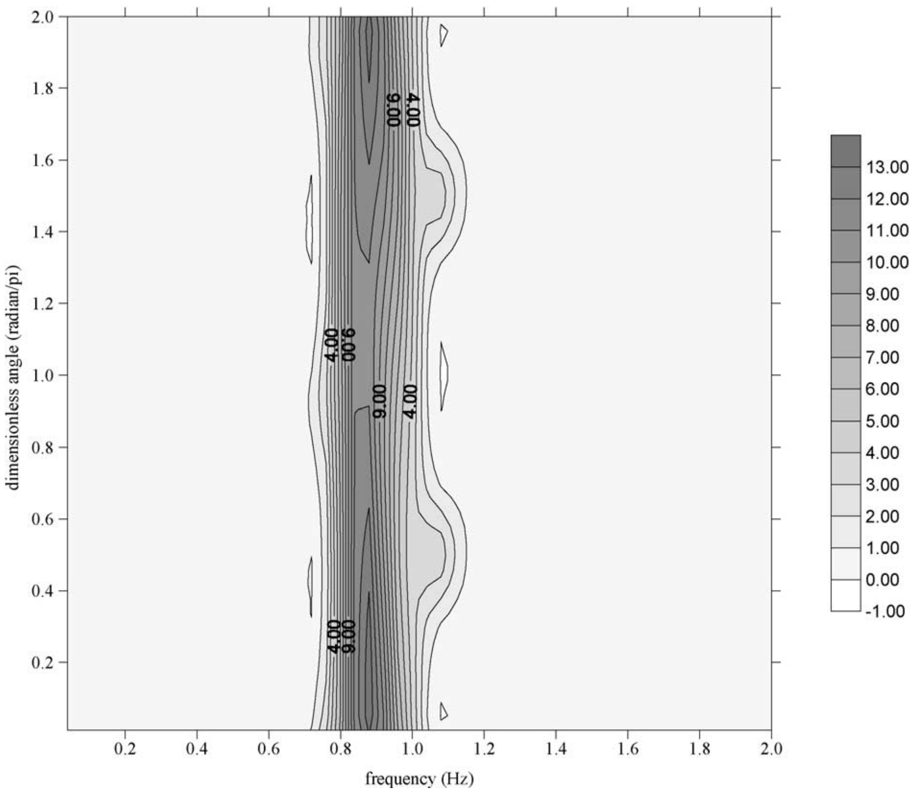

Fig. 6. Contour of the directional spectrum estimated by the EMEP that was affected by phase-locking.

distance (D) to the dominant wavelength (WL). The latter is calculated from the dispersion relationship using the peak frequency of the spectrum.

The reflection coefficients decreased rapidly within four wavelengths away from the detached breakwater and tend to reach a constant value after four wavelengths. This is a similar trend to that mentioned earlier, that is as the waves became more and more long-crested, reflections will be more and more pronounced within the region of four wavelengths, can also be detected from the table. When the measuring distance has exceeded four wavelengths this tendency no longer holds.

In Fig. 5 we have plotted all the reflection coefficients estimated by the EMEP from the experiments. It can be seen from the figure that the reflection coefficients seem to have no definite relationships to either wave directionality or the distance when the measuring sites are located more than four wavelengths away from the detached breakwater. And the reflection coefficients seem to approach to a constant value. Within four wavelengths from the detached breakwater, the rate of the decrease is faster for wave fields having smaller directional spreads. Goda (2000) pointed out that the length of the crest lines of the reflected waves is limited by the length of the reflector. Therefore, the reflected waves disperse during propagation away from the source of reflection in a manner similar to the phenomenon of wave diffraction. Since the length of the detached breakwater is fixed, the length of the crested lines of reflected waves varied with the spreading parameter. As the waves became shorter crested, reflected waves would disperse wider and lesser reflected energy would travel through the measurement points.

When the distance (D) is within the range of one wavelength, there are cases where the estimated reflection coefficients have values larger than 1. It is unrealistic that energies of the reflected waves should have values larger than that of the incident waves. As

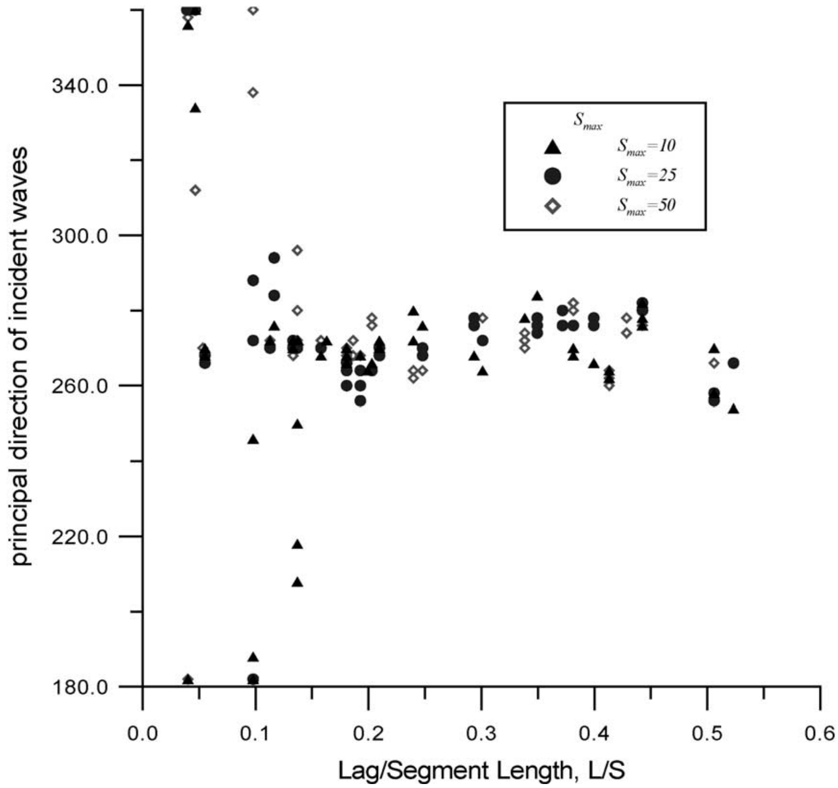

Fig. 7. Principal direction of the incident waves.

pointed out earlier, for a wave field in front of the reflector, standing waves are formed and there are nodes and antinodes. It is conjectured that some of the wave gauges are located near those points. When this is the case, measured surface elevations would have been contaminated. As a result, the vital phase information between wave gauges, which are need for the estimation of directional spectrum, are then obscured. Under these circumstances, the directional spectrum, estimated by the EMEP method showed that the wave energy would be scattered in the directional band. Bococtti et al. (1993) have studied the reflecting of wind wave fields in front of a reflecting wall. He found that the nodes and the antinodes tend to disappear starting one wavelength away from seawall. This is also seen in our estimation of the directional spectra. It is seen that when D/WL is greater than 1, reasonable estimates of the spreading of energy can be achieved.

Fig. 6 shows the contour plot of the directional spectrum estimated by the EMEP affected by phase-locking. The ratio of D/WL is 0.5, within the region that the value is lesser than 1, the effects of standing waves, as well as nodes and antinodes, are dominant. The star array is located at 1 m away from the detached breakwater. The peaks in the spatial domain of the incident and reflected waves are invisible. The principal directions that the incident and reflected waves propagate can only be distinguished in the frequencies that are higher than the peak frequency. The energy is spread all over in regions near the peak frequency. Thus, it leads to the errors in estimating reflection coefficients.

4.3. Effect of time ratio of measurement

Huntley and Davidson (1998) suggest that, if MLM were used in a reflective wave field, the time

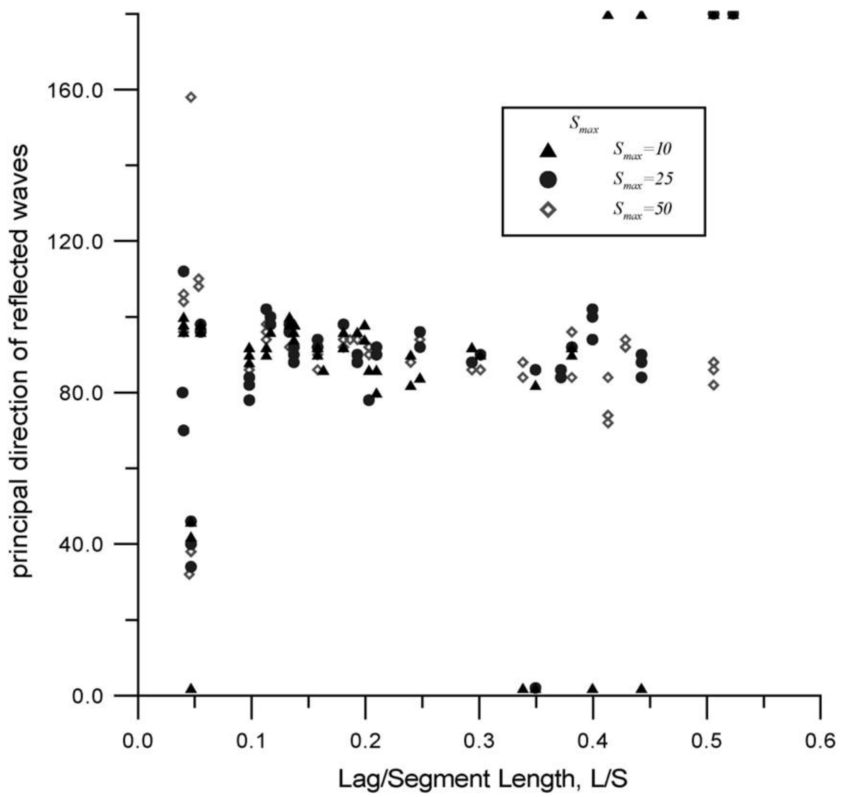

Fig. 8. Principal direction of the reflected waves.

ratio L/S should greater than 0.5. We studied the minimum L/S ratio for the EMEP method. The method is said to be applicable, when the principal directions of both the incident and reflected waves can be separated clearly. All of our experiments have ratios of L/S less than 1, which means that all the measurements were carried out in regions where the effects of phase locking are predominant. Fig. 7 shows the estimated principal directions of the incident waves by the EMEP method. For all cases, the waves should have energies concentrated in 270°, which is normal to the detached breakwater. It can be seen that, the majority of the estimated results are distributed along the target one. However, when the ratios of L/S were less than 0.15, the estimated results begin to deviate from the target.

Fig. 8 shows the principal directions of the reflected waves. Reflected waves will propagate at an angle which is equal to that of the incident waves but opposite in direction. Estimated principal directions of the reflected waves are seen to be distributed around 90° until L/S less than 0.1. That is to say that the non-phase-locked method, such as EMEP, can predict the principal directions of the incident and reflected waves correctly until the ratio L/S is less than 0.15. This is apparently larger than those of the less exact method such as MLM. It is also interesting to note that estimated results are less affected by the values of the spreading parameter.

5. Conclusions

Two methods for the estimation of directional spectrum, the EMEP and the MLM, were used here to test their capabilities in estimating reflective wave fields. Generally speaking, the former outperforms the latter in that the spurious peaks occur lesser. For distances away from the breakwater, a reflection line is not needed as input.

The results indicate that within a distance of four dominant wavelengths to the detached breakwaters, the reflection coefficient increases with increasing magnitudes of the spreading parameter and decreases with increasing distance away from the detached breakwater. On the other hand, for distances more than four dominant wavelengths away from the breakwater, the reflection coefficient seems to approach to a constant value and has no specific relationship with the wave directionality and measuring distance. However, for a distance less than one dominant wavelength from the detached breakwater, this method fails to estimate the directional spectrum in some cases. The effects of standing waves are severe in this region and estimated cross spectra between wave gauges become less accurate.

Our results indicate that even the time ratio of L/S is as small as 0.15, the use of more exact non-phase locked estimation method such as EMEP can still be used. This ratio is much smaller than that proposed by Huntley and Davidson (1998).

References

Boccotti, P., Barraro, G., Fimma, V., Mannio, L., Rotta, A., 1993. An experiment at sea on the reflection of the wind waves. Ocean Engineering 20 (5), 493–507.

Briggs, M.J., Thompson, E.F., Vincent, C.L., 1995. Wave diffraction around breakwater. Journal of Waterway, Port, Coastal and Ocean Engineering 121, 23–35.

Brissette, P., 1992. Estimation of wave directional spectra and application to the study of surface gravity water waves. PhD Thesis, McMaster University, Canada.

Chadwick, A.J., Pope, D.J., Borges, J., Ilic, S., 1995. Shoreline directional wave spectra: Part 1. An investigation of spectral and directional analysis techniques. Proceedings of Institution of Civil Engineering in WaterMaritime and Energy, vol. 112, pp. 198–209.

Davidson, M.A., Huntley, D.A., Bird, P.A.D., 1998. A practical method for the estimation of directional wave spectra in reflective wave fields. Coastal Engineering, Elsevier 33, 91–116.

Davidson, M.A., Kingston, K.S., Huntley, D.A., 2000. New solution for directional wave analysis in reflective wave fields. Journal of Waterway, Port, Coastal and Ocean Engineering, 173–181.

Elgar, S., Herbers, T.H.C., Guza, R.T., 1994. Reflection of ocean surface gravity waves from a natural beach. Journal of Physical Oceanography 24, 1503–1510.

Frigaard, P., Helm-Petersen, J., Klopman, G., Stansberg, C.T., Benoit, M., 1997. IAHR list of sea state parameters. Proceedings of the Twenty-seventh IAHR Congress, Seminar: Multi-Directional Waves and their Interaction with Structures, San Francisco, 15–19.

Gaillard, P., Gautheir, M., Holly, F., 1980. Method of analysis of random wave experiments with reflecting coastal structures. Proceedings of the 17th Coastal Engineering Conference, ASCE, pp. 204–220.

Goda, Y., 2000. Random Seas and Design of Maritime Structures, 2nd ed. University of Tokyo Press, Tokyo, pp. 31–103.

Goda, Y., Suzuki, Y., 1976. Estimation of incident and reflected waves in random wave experiments. Proceedings of the 17th Coastal Engineering Conference, ASCE, pp. 828–845.

Hashimoto, N., 1997. Analysis of the directional wave spectrum from field data. Advanced in Coastal and Ocean Engineering, World Scientific 3, 103–143.

Hashimoto, N., Kobune, K., Kameyama, Y., 1987. Estimation of directional spectrum using the Bayesian approach, and its application to field data analysis. Report of the Port and Harbour Research Institute 26, 57–100.

Hashimoto, N., Nagai, T., Asai, T., Sugahara, K., 1993. Extension of the maximum entropy principle method for estimating directional ocean wave spectrum. Report of the Port and Harbour Research Institute 32 (1), 3–25 (In Japanese).

Huntley, D.A., Davidson, M.A., 1998. Estimating the directional spectrum of waves near a reflector. Journal of Waterway Port, Coastal and Ocean Engineering 124 (6), 312–319.

Ilic, S., Chadwick, A.J., Davidson, M.A., Bird, P.A.D., Huntley, D.A., 1997. Directional analysis of partially reflected waves. Proceedings of the 27th IAHR Congress, Seminar: Multidirectional Waves and their Interaction with Structures, San Francisco, 323–336.

Ilic, S., Chadwick, A., Helm-Petersen, J., 2000. An evaluation of directional analysis techniques for multidirectional, partially reflected waves. Part 1: Numerical investigations. Journal of Hydraulic Research 38 (4), 243–251.

Isobe, M., Kondo, K., 1984. Method for estimating directional wave spectrum in incident and reflected wave field. Proceedings of the 19th International Conference on Coastal Engineering, ASCE, pp. 467–483.

Kondo, K., Akama, M., Isobe, M., 1986. Measurement of reflection coefficient of sea wall in Omura bay. Proceedings of the 20th Coastal Engineering Conference, ASCE, pp. 1987–2001.

Nwogu, O., 1989. Analysis of fixed and floating structures in random multi-directional waves, PhD Thesis, University of British Columbia, Vancouver, BC, Canada.

Yokoki, H., Isobe, M., 1996. A method for estimating directional spectra in a field of incident and reflected waves. Proceedings of the 25th Coastal Engineering Conference, ASCE, pp. 43–54.